Fatigue Crack Path through Cast Al-Si Alloy Microstructure

R. Konečná[1], S. Fintová[1] and G. Nicoletto[2]

[1] Department of Materials Engineering, Faculty of Mechanical Engineering, University of Žilina, Univerzitná 1, 010 26 Žilina, Slovak Republic,
radomila.konecna@fstroj.uniza.sk
[2] Department of Industrial Engineering, University of Parma, Viale G.P. Usberti, 181/A, 43100 Parma, Italy

ABSTRACT. *Casting defects favor early fatigue crack initiation strongly dependent on the initiating pore size and shape. This paper reports a study, in which specimens extracted from real castings and used for high-cycle rotating bending fatigue testing were examined with metallographic techniques. The Murakami's statistical method based on the largest extreme value distribution was used for the statistical description of the pore size population observed on metallographic cross-sections. The largest defect sizes occuring in real castings were predicted by this statistical method. The fatigue fracture surfaces of the specimens were observed by scanning electron microscopy (SEM) and the fatigue crack initiation places identified. After the fatigue crack initiation also the cracks propagation was examined and the crack paths were determined. Fracture mechanics based predictions were compared to experimental results.*

INTRODUCTION

Cast aluminum alloys are widely used in fatigue critical structural components of the automotive industry to reduce fuel consumption. Typical applications are engine blocks, cylinder heads, chassis and suspension components, [1]. Cast Al-Si alloys are characterized by microstructural features such as secondary dendrite arm spacing (SDAS) and the sizes of eutectic silicon and intermetallic particles. Formation of porosity and microshrinkage cavities are almost inevitable in the sand casting process [1] and are the most detrimental for the fatigue behavior. Typically, fatigue endurance is reduced when the size of porosity increases [2 - 9] because not only fatigue crack propagation is reduced but also the initiation period is accelerated.

Since porosity is assumed to reduce the crack initiation phase by creating a high stress concentration in the material adjacent to the pores, damage-tolerant approaches to the fatigue design of cast aluminum components are based on fracture mechanics calculations using the "long crack" behavior described by threshold ΔK_{th} and Paris's law, [3, 7, 9, 11]. It assumes the presence of casting defects and assesses part performance based on crack propagation because the crack initiation phase from a pore is expected to add a negligible contribution to the total fatigue life.

However, Ferrie et al. [10] demonstrated using high resolution synchrotron radiation X-ray microtomography that a substantial part of the lifetime (25 % of the total estimated fatigue life) is required for the crack to surround the pore and assume a semi-elliptical shape. Therefore, fracture mechanics may give lower-bound fatigue life predictions unless the role of local microstructure (i.e. eutectic structure and intermetallic phases) on crack initiation and early development is included. McDowell and al. [12] determined the cyclic plastic deformation concentration depending particle morphology and distribution near a pore. Lados and Apelian [13] showed that short fatigue cracks follow paths that connect reinforcing particles.

Since the decrease in fatigue life is directly correlated to the increase of initiating pore size, a practical method to describe the defect population and its size distribution from empirical data is needed to proceed with defect tolerant design approach. The authors, [14, 15], have been examining the potential of the extreme-value statistics to estimate the maximum pore size in cast Al-Si alloys based on metallographic data.

In the present contribution high-cycle rotating bending fatigue specimens of a cast AlSi7Mg alloy that failed because cracks initiated at casting pores at or near the surface are metallographically prepared to investigate crack propagation from the pore size to the final crack length at fracture. The present work is aimed to find the correlation between the sizes of defects observed on fatigue fracture surfaces and the defect size estimates obtained by metallographic characterization of pore size population. A critical pore size is then used in life prediction with fracture mechanics.

EXPERIMENTAL PROCEDURES

Material and Microstructure

Cast AlSi7Mg is the alloy investigated for its technical importance in the automotive industry. Material used here was extracted from actual cast parts.

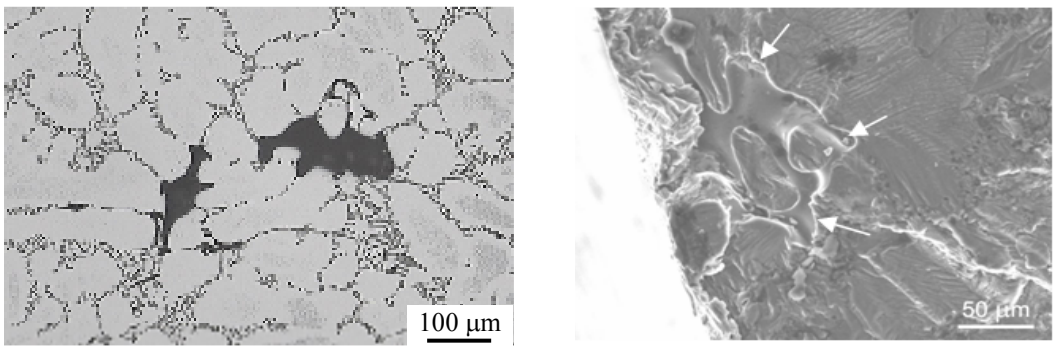

a) b)

Figure 1. a) typical shrinkage casting pores and microstructure
b) typical ramificated fatigue crack initiating pore

Microstructural characterization considered average SDAS and grain size. Size, shape factor and distribution of eutectic Si particles were also determined. A typical microstructure, shown in Fig. 1a, is characterized by primary dendrites of α-phase. Eutectic (α + Si) silicon particles and intermetallic phases were located between the secondary dendrite arms. An average SDAS of 60 μm was common to all casts. Fig. 1a shows also typical shrinkage casting pores affecting fatigue resistance.

Fatigue Testing and Analysis

Smooth 6-mm-diameter fatigue specimens made of AlSi7Mg alloy were tested under rotating bending loading at 50 Hz with the aim of fatigue strength at 10^7 cycles. Smooth 6-mm-diameter push-pull fatigue specimen were subsequentially extracted from the broken halves of the bending specimens and tested in an Amsler vibrophore to determine the influence of the loading mode on fatigue strength. All fatigue fractures were initiated at casting pores.

Fatigue fracture profiles were prepared to optically determine crack path features that explain the link between critical pore, microstructure and path direction. Fracture surfaces of selected specimens were also investigated in the SEM to determine critical pore sizes that originated the fatigue crack. One example is in Fig. 1b.

Largest Pore Size Statistics using Metallography

Damage tolerant calculations require the definition of a representative initial crack size, which could be related to a significant pore size. This parameter is expected to depend on the part geometry, casting process parameters and chemical composition. Furthermore, porosity is not uniformly distributed within a cast part. An indication of local material quality and a representative initial crack size in the material volume derive from a description of pore size population.

Random metallographic 2-D sections of pores cannot provide estimates of their largest defect size and the pores observed will not be the largest in the part. Therefore, the maximum pore size in a cast component can only be estimated by extrapolation of the statistical description of the equivalent pore sizes obtained by metallography. The equivalent crack-like measure of pore severity was assumed to be $(A)^{1/2}$ where A is the pore area determined by optical inspection. Murakami's method was applied to the characterization of the pore size population according the largest extreme value distribution (LEVD), [16, 17] based on the evaluation of the largest defect size in many (at least 20) fields of view. The image analysis program LUCIA Metallo 5.0 was applied for extensive and detailed measurement of largest pores on a specimen-to-specimen basis.

RESULTS AND DISCUSSION

Fatigue tests

The present fatigue results in push-pull and rotating bending are shown in Fig. 3 (i.e. filled symbols). Multiple run-out at 10^7 cycles are also identified in the plot. The fatigue

strength at 10^7 cycles and 50 % probability for push-pull loading was determined to be Sa,pp = 50 MPa and standard deviation s = 4.5 MPa and for rotating bending Sa,rb = 65 MPa and s = 9.3 MPa. The present push-pull fatigue test data correlate with analogous data for A356-T6 from the literature, [5].

All fatigue fractures plotted in Fig. 2 initiated at a casting pore on the surface or just below such as that shown in Fig. 1b because of the rotating bending loading that develops the highest stress on and near the surface. The fractographic analysis showed also that is multiple fatigue crack initiations. The effective defect size of the critical pore was obtained by measuring the area of the pore contour. The square root of the area $(A)^{1/2}$ are summarized in Tab. 1 with the largest critical pore sizes for each fracture surface in bold.

Table 1. Fatigue results and determination of the largest initiation pore size

Specimen	**S [MPa]**	**Experimental N_f [cycles]**	**Observed initiation pore sizes [µm]** (multiple initiatons)	**Predicted largest pore size for S = 10 mm^2 [µm]**	**Predicted N_f [cycles]**
3B	80	2 074 770	60; **88**	143	249400
5B	70	669 562	**97**; 88; 48; 47; 84	87	422400
6B	60	870 745	36; **82**; 50	120	774700

Fatigue crack paths

A typical composite image of a crack profile is shown in Fig. 3a. Inspection of the high magnification micrograph shows the path of the fatigue crack through the microstructure.

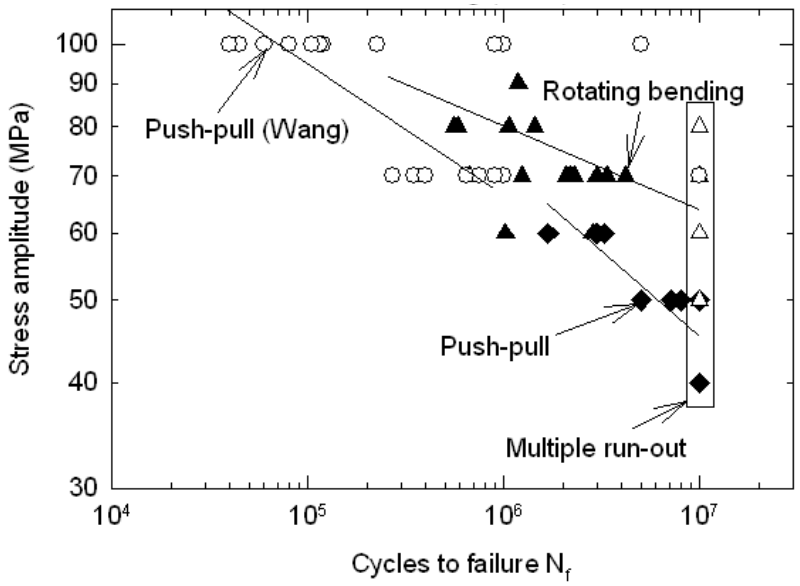

Figure 2. Fatigue data for cast AlSi7Mg alloys obtained by push-pull and rotating bending

Since crack initiated from a cast pore, the left side shows growth near the critical pore (enlarged view in Fig. 3b). The initiation phase is influenced by Si particles, which are found at reentrant corners of the pore and a fractured Si particle is observed.

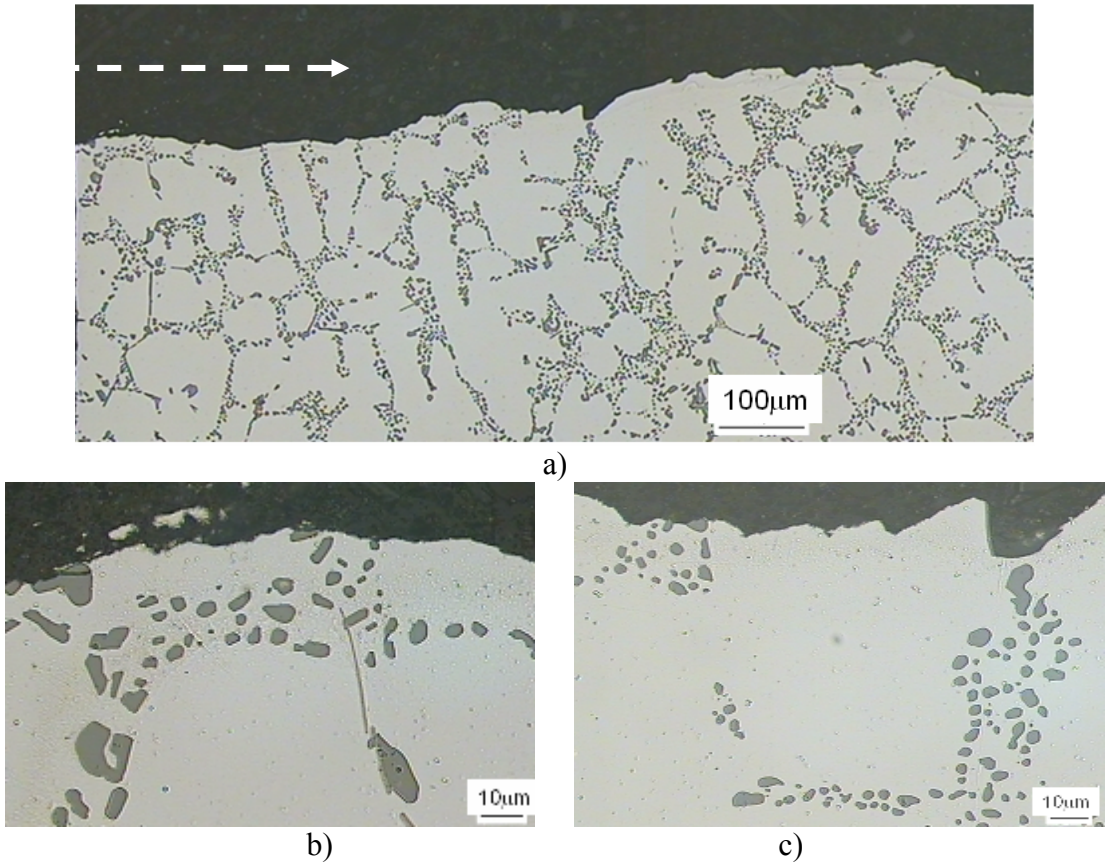

a)

b)

c)

Figure 3. Fatigue crack path a) global view;
b) near initiation point c) low ΔK propagation

As the crack propagates, the Si particles appear not to affect crack direction. At low ΔKs, crack propagation through the α–phase shows crystallografic propagation producing crack surface roughness, (see Fig. 3c).

At ΔK increases, crack propagation becomes more affected by eutectic Si particle clusters. Mode I fatigue crack propagation is followed by quasi static crack advances as shown in the left side of Fig. 4a. At final rupture, the crack propagates along a zig-zag path through regions rich of Si particles. Locally, lamellas of intermetalic phase $FeSiAl_5$ activate cleavage on their interface with the alpha phase (see Fig. 4b). The present observations confirm the crack deflection pattern models proposed by Lados, [13].

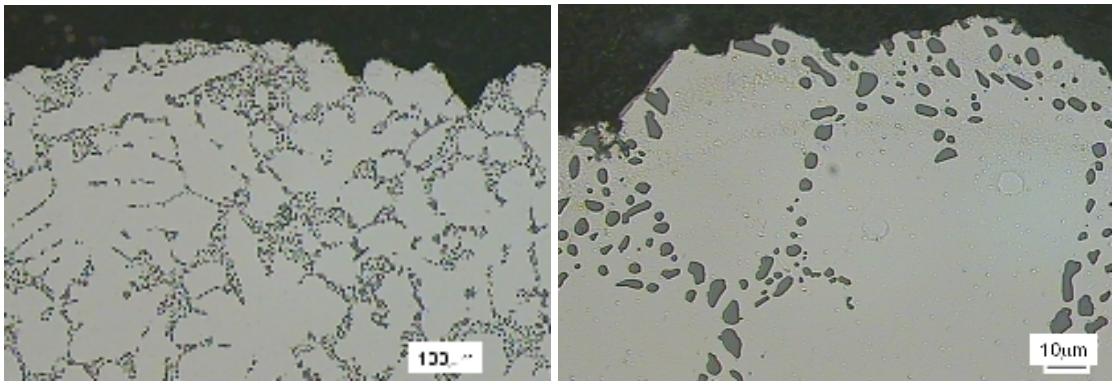

a) b)

Figure 4. Fatigue crack path a) high ΔK and static fracture;
b) crack and Si particles

LEVD Distributions

The results of the largest pore size characterization according to the LEVD method, [16], for several fatigue specimens are plotted in Fig. 5. The control measurement area was $S_0 = 1.86$ mm^2. The data show that the linearity requirement for the applicability of LEVD is only partially satisfied. In many cases an inflection point at a pore size discriminating small pore from large fatigue-critical pores is observed. Such inflection points are associated to the pore sizes 30 ÷ 40 µm suggesting that pores above and below this threshold size distribute differently. A threshold defect size for fatigue crack initiation of 50 µm was also introduced in [6]. The specimem-to-specimen variation of the data of Fig. 5 is due to their being extracted from different parts of the casting.

To initially test the possibility to extract size estimates for fatigue life calculations, selected LEVD distributions of Figure 5 were used to predict the largest pore size in the

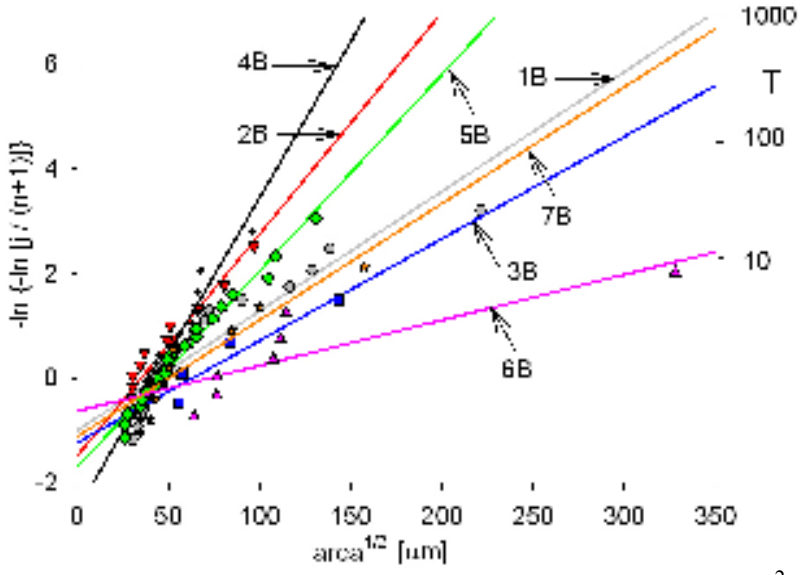

Figure 5. LEVD plots of equivalent pore size ($S_0 = 1.86$ mm^2)

specimens as shown in Table 1. These predicted sizes are compared to the critical pore sizes observed by SEM inspection of the actual fracture surfaces. An extrapolation of the largest pore size expected in a cross-sectional area of $S = 10\,mm^2$, which is representative of the highly stressed specimen area of the specimen under bending load, was perfomed according to the return period T approach, [16]. The predicted sizes are shown in Table 1 with the fatigue data. The predicted critical pore sizes overestimate the sizes of the largest defects observed on fatigue fracture surfaces therefore on the safe side. On the other hand the condition of multiple crack initiation and crack interaction could not be forecast and may have a role on the fatigue life.

Fatigue life estimates

The assumption behind the pore size characterization with metallography is that fatigue life and fatigue strength decrease with an increasing expected largest pore size. A fatigue model is needed to proceed with the fatigue life estimate starting from the initial crack size. Linear elastic fracture mechanics principles are used to evaluate the influence of porosity on the fatigue limit and voids and shrinkage at the place of crack initiation are assumed as initial cracks. Following Murakami et al. [16] the stress intensity factor mainly depends on the area of the flaw and its location and is influenced by its shape by less than 10 %. With this assumption, the stress intensity amplitude, K_{max} is calculated for R = -1, [16] as

$$K_{max} = \sigma_{max} \cdot \alpha \cdot (\pi A^{1/2})^{1/2} \quad (1)$$

where σ_{max} is the stress amplitude, α is the geometry factor for a surface crack in a round bar in bending. The integration of Paris law for a semicircular surface crack having the size of the pore was performed numerically using the following material constants m = 3.85 and $C = 4.458\ e^{-12}$ $(MPa\ m^{1/2})^{-m}$, [9]. The fatigue life estimates of Table 1 are for an iniatial crack size of 100 μm, which is a representative size of both the observed and predicted largest pore sizes of Table 1. Obviously, the predicted fatigue lives reduce with increasing applied stress, which is not the case from the experiments. However, the role played by multiple initiations is not clear in the experiments. Compared to the rotating bending fatigue data of Fig. 2, these predictions provide a lower-bound fatigue response.

CONCLUSIONS

The following conclusions are reached from this study:

- The fatigue cracks in rotating bending specimens were initiated from casting pores on the free surface or just below the surface.
- The fatigue crack path is initially influenced by the silicon particles near the critical pore then grows straight through the alpha phase. At high growth rates the crack path becomes irregular and links rows of silicon particles.

- Murakami's method for largest pore size statistical description using LEVD and metallographic inspection was applied on a specimen-to-specimen basis thus showing a threshold pore size for fatigue initiation.
- Critical pore sizes on fatigue fracture surfaces are compatible to initial pore sizes predicted by the LEVD description.
- Initial life predictions using long crack fracture mechanics showed reasonable lower bound capability.

ACKNOWLEDGEMENTS

This work was performed as a part of VEGA grant No.1/3194/06 and KEGA grant No.3/6110/08 and within the objectives of MATMEC, Emilia-Romagna regional net-lab (http://www.matmec.it/).

REFERENCES

1. Kaufman, J.G, Rooy, E. L. (2004) *Aluminum Alloy Castings - Properties, Processes and Applications*, AFS/ASM International.
2. Sonsino, C.M., Ziese, J. (1993) *Int. J. Fatigue*, **15,** 75-82.
3. Dabayeh, A.A., Xu, R.X., Du, B.P. and Topper, T.H. (1996) *Int. J. Fatigue*, **18**, 95-104.
4. Caton, M.J., Jones, J.W., Boileau, J.M. and Allison, J.E. (1999) *Metall. Mater. Trans. A*, **30A**, 3055-68.
5. Wang, Q.G., Apelian, D. and Lados, D.A., (2001) *J. Light Met*., **1**, 85-97.
6. Buffiere, J-Y., et al. (2001) *Materials Science and Engineering,* **A316**, 115–126.
7. Mayer, H., Papakyriacou, M., Zettl, B. and Stanzl-Tschegg, S.E. (2003) *Inter J Fatigue*, **25**, 245–256.
8. Wang, Q.G., Jones, P.E., (2007) *Metall. Mater. Trans. B*, **38B**, 615-621.
9. Lados, D.A., Apelian, D. and Donald, J.K. (2006) *Acta Mater*. **54** (6), 1475-1486.
10. Ferrie, E., Buffiere, J.-Y., Ludwig, W., (2005) *Int. J. Fatigue,* **27**, 1215–1220.
11. Gao, Y.X., Yi, J.Z, Lee, P.D. and Lindley, T.C., (2004) *Fatigue Fract Engng Mater Struct*, **27,** 559-570.
12. Gall, K., Yang, N., Horstemeyer, M., McDowell, D.L., and Fan, J. (1999) *Metall. Mater. Trans.* A **30A**, 3079-3088.
13. Lados, D.A., Apelian, D. (2006) Int. Conf. Crack Path CP06, Parma, Italy, Paper # 026 in Procs. CD.
14. Nicoletto, G., Konečna, R, Baicchi, P, Majerova, V. (2008). *Materials Science Forum*, **567-568**, 393-396.
15. Baicchi, P., Nicoletto, G., Riva, E. (2006). *Procs Crack Paths* (CP 2006). Parma.
16. Murakami, Y. (2002) *Metal Fatigue: Effects of Small Defects and Nonmetallic Inclusions*, Elsevier, Oxford.
17. Beretta, S., el al. (1997) *Int. J. Fatigue*, **19**, 319-33.